EuroIntervention 2019;15:722-730 published online May 2019

Pulmonary artery denervation using catheter-based ultrasonic energy

Alexander Rothman[1]*, BMBCh, PhD; Michal Jonas[2], MD; David Castel[3], MD; Abraham Rami Tzafriri[4], PhD; Hannes Traxler[5], MD; Dalit Shav[6], PhD; Martin Leon[7], MD; Ori Ben-Yehuda[8], MD; Lewis Rubin[9], MD

1. Infection, Immunity and Cardiovascular Disease, University of Sheffield, Sheffield, United Kingdom; 2. Department of Cardiology, Kaplan Medical Center, Hebrew University School of Medicine, Rehovot, Israel; 3. Neufeld Cardiac Research Institute, Sheba Medical Center, Tel Hashomer, Israel; 4. CBSET Inc, Lexington, MA, USA; 5. Center of Anatomy and Cell Biology, Medical University Vienna, Vienna, Austria; 6. SoniVie, Rosh Haayin, Israel; 7. Columbia University Medical Center, NY, USA; 8. Cardiovascular Research Foundation, NY, USA; 9. University of California, San Diego, CA, USA

This paper also includes supplementary data published online at: https://eurointervention.pcronline.com/doi/10.4244/EIJ-D-18-01082

KEYWORDS

- innovation
- preclinical research
- pulmonary hypertension

Abstract

Aims: Pulmonary arterial hypertension is a devastating disease characterised by pulmonary vascular remodelling and right heart failure. Radio-frequency pulmonary artery denervation (PDN) has improved pulmonary haemodynamics in preclinical and early clinical studies; however, denervation depth is limited. High-frequency non-focused ultrasound can deliver energy to the vessel adventitia, sparing the intima and media. We therefore aimed to investigate the feasibility, safety and efficacy of ultrasound PDN.

Methods and results: Histological examination demonstrated that innervation of human pulmonary arteries is predominantly sympathetic (71%), with >40% of nerves at a depth of >4 mm. Finite element analysis of ultrasound energy distribution and *ex vivo* studies demonstrated generation of temperatures >47ºC to a depth of 10 mm. In domestic swine, PDN reduced mean pulmonary artery pressure induced by thromboxane A2 in comparison to sham. No adverse events were observed up to 95 days. Histological examination identified structural and immunohistological changes of nerves in PDN-treated animals, with sparing of the intima and media and reduced tyrosine hydroxylase staining 95 days post procedure, indicating persistent alteration of the structure of sympathetic nerves.

Conclusions: Ultrasound PDN is safe and effective in the preclinical setting, with energy delivery to a depth that would permit targeting sympathetic nerves in humans.

**Corresponding author: Department of Infection, Immunity and Cardiovascular Science, University of Sheffield, The Medical School, Beech Hill Road, Sheffield, S10 2RX, United Kingdom. E-mail: a.rothman@sheffield.ac.uk*

SUBMITTED ON 14/11/2018 - REVISION RECEIVED ON 19/03/2019 - ACCEPTED ON 03/05/2019

DOI: 10.4244/EIJ-D-18-01082

Abbreviations

H&E	haematoxylin and eosin
mPAP	mean pulmonary artery pressure
PAH	pulmonary arterial hypertension
PDN	pulmonary artery denervation
PH	pulmonary hypertension
RF	radio-frequency
SD	standard deviation
SEM	standard error of the mean
SG	Swan-Ganz catheter
TH	tyrosine hydroxylase
TxA2	thromboxane A2

Introduction

Pulmonary arterial hypertension (PAH) is a complex disorder characterised by increased pulmonary vascular resistance and right heart failure. Current therapies provide benefit through modulation of the prostacyclin, endothelin-1 and nitric oxide pathways[1]; however, patients continue to experience significant morbidity and mortality[2].

Sympathetic and neurohormonal activity including plasma norepinephrine[3,4], muscle sympathetic nerve activity[5,6] and indicators of renin–angiotensin–aldosterone system[7] activity are increased in patients with PAH and are associated with adverse clinical outcome[4-6]. Modulation of the sympathetic and renin–angiotensin–aldosterone systems is an established treatment for heart failure[8-13]. Both beta-blockers[14,15] and angiotensin-converting enzyme inhibitors[7] have been shown to attenuate disease in experimental models; however, there is no evidence of benefit in patients with PAH[16-18].

Preclinical studies have demonstrated that pulmonary artery denervation (PDN) improves pulmonary haemodynamics in acute[19,20] and chronic models of pulmonary hypertension (PH)[21] and in a single-centre study of patients with PAH[22]. A single case report used high-output burst electric stimulation applied within the pulmonary artery to induce autonomic responses[23]; however, the distribution of nerves around the pulmonary arteries in humans remains largely unknown. We therefore examined nerve distribution around the pulmonary arteries in humans and, using a novel ultrasound energy delivery system, we sought to demonstrate histological evidence of a thermal effect on pulmonary artery adventitial nerves and a haemodynamic effect in an acute vasoconstrictive model of PH.

Editorial, see page 659

Methods

HUMAN PULMONARY ARTERY NERVE DISTRIBUTION

Human cadavers and histological samples were examined to determine the distribution of pulmonary artery innervation.

CADAVERIC

Anatomical examination was conducted at the Vienna Medical University, Austria, in accordance with European Commission (EC) approval (1424/2015). The rib cage was lifted to allow inspection of the thoracic anatomy of two cadavers (1 male and 1 female). The pulmonary artery (PA) dimensions, distance to major structures and nerve supply were determined by anatomical inspection.

HISTOLOGICAL

The pulmonary arteries were excised *en bloc* and stained as previously described[20], using rabbit anti-tyrosine hydroxylase antibody (1:300, AB152; Merck Millipore, Burlington, MA, USA) and neurofilament (1:500, Ab24574; Abcam, Cambridge, United Kingdom) primary antibodies with species-specific secondary antibodies. Nerve location, area and distance from the vessel lumen were measured. Consecutive slides were projected onto a Cartesian map to form a two-dimensional (2D) representation of the nerve distribution. The data presented represent the distribution of individual nerves in the patients examined.

COMPUTATIONAL MODELLING: FINITE ELEMENT ANALYSIS

A simplified simulation of induced heat in tissue following ultrasound energy delivery was performed using 2D Cartesian numerical models (MATLAB R2009; MathWorks, Natick, MA, USA).

A constant diffusion coefficient per tissue type was assumed through time and piecewise constant through space reducing the equation to:

$$\rho C_P \frac{\partial T}{\partial t} = \underbrace{k\left[\frac{\partial^2 T}{\partial x^2}+\frac{\partial^2 T}{\partial y^2}\right]}_{diffusion} + \underbrace{q_s}_{\substack{creation\\in\ tissue}} - \underbrace{\rho C_P\left[u\frac{\partial T}{\partial x}+v\frac{\partial T}{\partial y}\right]}_{advection} + \underbrace{q_u}_{\substack{ultrasonic\\absorption\\in\ tissue}} \quad [24]$$

T-temperature profile; ρ-density; C_P-capacity; q_s-metabolic heat generation; q_u-heat absorption ($q_u = Ie^{-\alpha(f)\vec{x}}$)[25]; I-intensity; α-attenuation coefficient; f-frequency; $\vec{x}$-position vector along the ultrasonic beam.

The model used a Crank-Nicolson method and comprised five concentric layers describing the region of interest geometry: lumen 25 mm, intima 0.02 mm, media 0.94 mm, adventitia 0.04 mm and perivascular tissue, with each layer defined by density, heat capacity, conductivity, metabolic heat generation and volumetric blood perfusion[25]. Transducer frequency was 11 MHz with an artery attenuation level of 15 dB/cm and coagulation necrosis threshold of 47°C. Transient effect was assumed to be negligible as tissue achieved steady state of >47°C in <3 seconds.

ULTRASOUND ENERGY DELIVERY EX VIVO

An ultrasound catheter (TIVUS; SoniVie, Rosh Ha'Ayin, Israel) was clamped submerged in a water bath and positioned using an XZY manipulator 8 mm from an *ex vivo* bovine liver sample. The three-directional ultrasound applicator of the catheter is a 2 mm diameter circumcircle of the equilateral triangle with a transducer of 6×1 mm on each side powered at 50 W/cm^2 with an operating frequency of 11 MHz.

ANIMAL STUDIES

Fifteen male swine were used for examination of the acute histological changes induced by PDN, seven to determine the haemodynamic efficacy of PDN and ten to determine the effects of PDN

at 14, 28 and 95 days. Anaesthesia was induced by intramuscular injection of ketamine (10 mg/kg), xylasin (2 mg/kg) and intravenous diazepam (1 mg/kg) and maintained with isofluorane 1.5-2.5% in 100% O_2 via endotracheal tube. Interventional procedures were performed with radiographic guidance (H-5000 Integris Cath Lab; Philips, Amsterdam, the Netherlands). Studies were conducted under ethical approval 950/14/ANIM from the Sheba Medical Center, Ramat Gan, Israel.

HAEMODYNAMIC MEASUREMENTS

Systemic and pulmonary pressures were measured using a 5.2 Fr pigtail catheter (Cordis, Cardinal Health, Milpitas, CA, USA) via a 6 Fr sheath in the femoral artery and a 7 Fr Swan-Ganz catheter (SG) (Edwards Lifesciences, Irvine, CA, USA) via an 8 Fr sheath in the right internal jugular vein (Cordis).

PULMONARY DENERVATION

PDN was performed using a multidirectional ultrasound catheter (TIVUS) and console **(Figure 1)**. Animals were randomised to PDN or a sham procedure (dummy catheter) undertaken via the internal jugular vein. Weight, HR and blood results are provided in **Supplementary Table 1**. The SG was advanced to the pulmonary artery and a 0.025"×260 cm wire (GuideRight™; St. Jude Medical, St. Paul, MN, USA) passed through the distal lumen; the SG was exchanged for a guiding catheter (RDC1; Cordis). The bifurcation of the main pulmonary artery and the ostium of the basal segmental branches were used as proximal and distal anatomic markers[20]. On a 0.014" wire, the TIVUS catheter was positioned and activated with the distancing mechanism open. Continuous monitoring of output and temperature with automated cut-out ensured that the ultrasound probe did not contact the vessel wall during activation. The number of activations was dependent on anatomy, limited to ten per vessel.

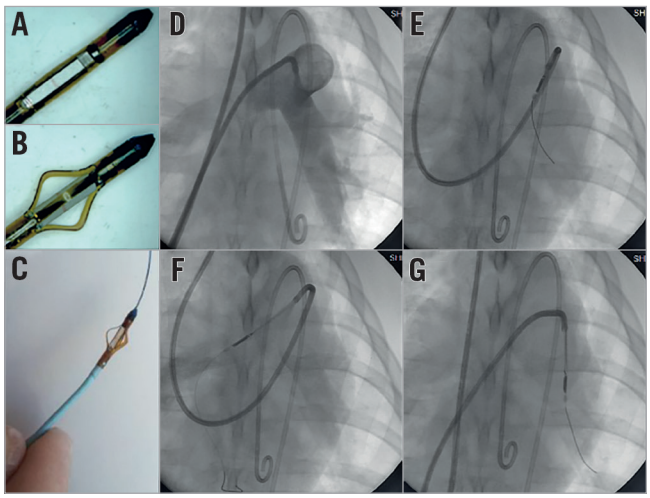

Figure 1. *TIVUS catheter. A) - C) Catheter with distancing device closed and open and on a 0.014" wire. D) Pulmonary angiogram. E) - G) Fluoroscopic images of the TIVUS catheter in right, main and left pulmonary arteries.*

THROMBOXANE-INDUCED PULMONARY HYPERTENSION

Acute PH was induced infusing thromboxane A2 agonist (TxA2, D0400; Sigma-Aldrich, St. Louis, MO, USA)[20,26] via a 6 Fr sheath in the right internal jugular vein. As previously described[20], the dose of infused TxA2 was increased at five-minute intervals, providing a dose-dependent increase in pulmonary artery pressure. Following the withdrawal of TxA2, pressure returned to baseline. PDN was then performed and TxA2 infused, identically to pre-treatment.

HISTOLOGICAL SCORING

Vessel scoring quantified endothelial loss, medial injury, inflammation, soft tissue injury and necrosis by light microscopy using H&E stained sections on a grading system (0=none; 1=minimal; 2=mild; 3=moderate; 4=severe)[27,28].

Nerve scoring quantified perineural inflammation or fibrosis and endoneural injury including vacuolisation, digestion chambers, pyknotic nuclei, and necrosis using a grading system (0=none; 1=minimal; 2=mild; 3=moderate; 4=severe)[27,28].

QUANTIFICATION OF SYMPATHETIC STAINING

Images of tyrosine hydroxylase (TH) stained sections were imported into ImageJ macOS X (NIH), threshold set, converted to greyscale and inverted for automated quantification of positive staining (CellProfiler 3.1.5macOS; Broad Institute)[29].

STATISTICAL ANALYSIS

Data are expressed as mean and/or SD. Differences were assessed by Student's t-test or Mann-Whitney test as appropriate in Prism 7.0d (GraphPad Software, San Diego, CA, USA).

Results

INNERVATION OF THE HUMAN PULMONARY ARTERIES

To determine the innervation of the pulmonary arteries and the proximity of local structures, anatomical and histological studies were undertaken in human cadavers. Macroscopic inspection demonstrated that the pulmonary plexus originated from the vagus nerve and the spinal ganglions. Parasympathetic nerves from the vagus were located caudal and anterior to the main pulmonary artery and sympathetic nerves from the spinal ganglions supplied the posterior aspect. Sympathetic and parasympathetic nerves merge to form a plexus, which was larger around the main pulmonary artery, splitting and reducing in size after the bifurcation of the main pulmonary artery. Other than intended targets, only the left recurrent laryngeal nerve was present within the 10 mm treatment area.

To define the distribution around the proximal pulmonary arteries, histological analysis evaluated nerve number and area. The number and area of nerves at the main pulmonary artery was greater than the left and right. Nerves were present at a depth of 1-12 mm with 44.7% and 46.2% surrounding the left and right pulmonary arteries at a depth >4 mm, respectively **(Figure 2, Supplementary Table 2)**. Seventy-one percent (71%) of nerves stained positive for TH, indicating a predominantly sympathetic innervation **(Supplementary Table 2)**.

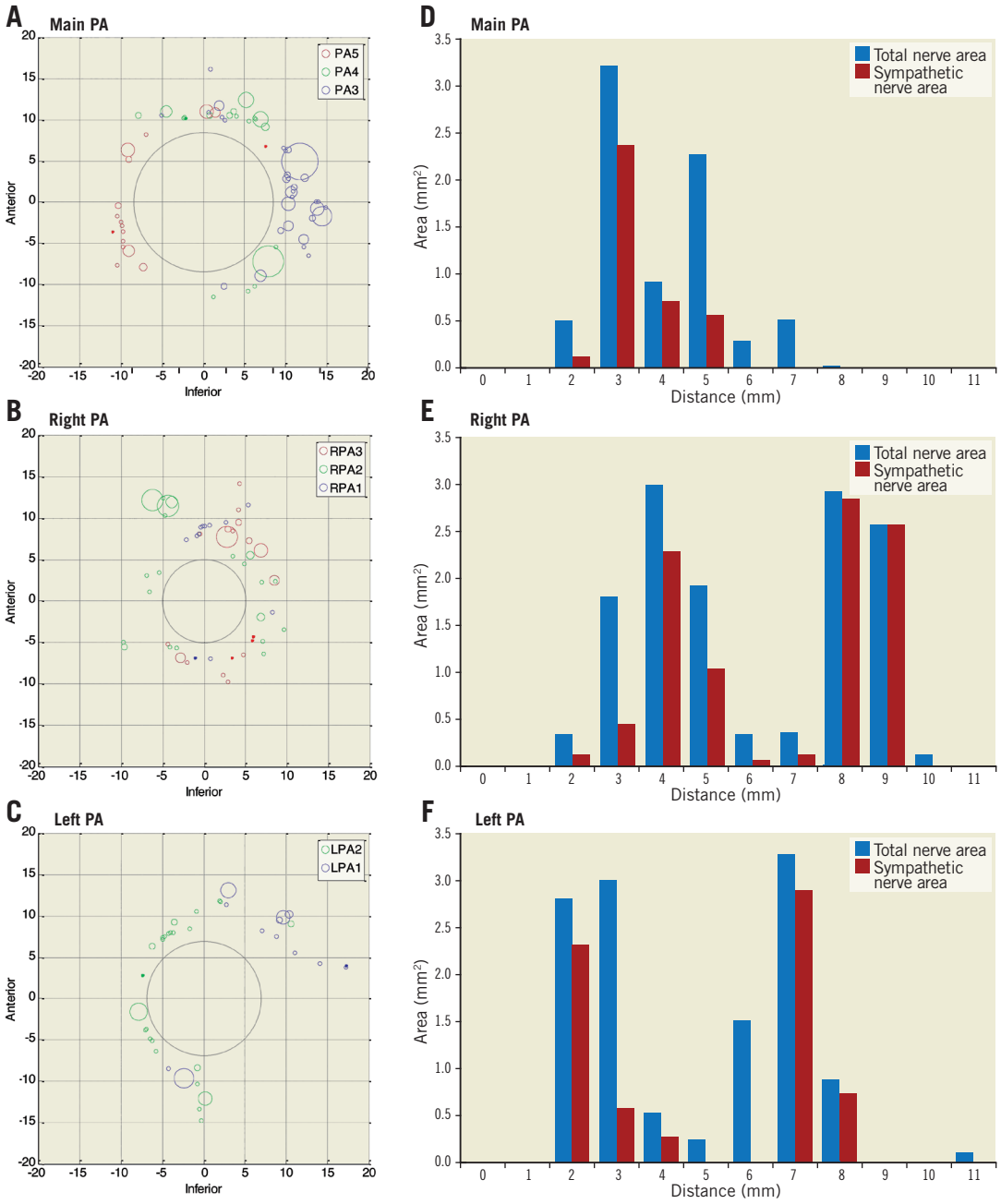

Figure 2. *Human pulmonary artery nerve distribution. A) - C) Cartesian representation of nerve distribution at the main, right and left pulmonary arteries in two patients at three sequential 3 mm sections (blue, green, red). Circles represent nerve area (mm). D) - F) Cumulative area and depth of sympathetic and total nerves from the luminal aspect of the pulmonary artery.*

COMPUTATIONAL SIMULATION OF ULTRASOUND ENERGY DELIVERY

Computational simulation of ultrasound energy delivery was used to model the effect on the pulmonary artery wall. **Figure 3A** shows computational modelling, suggesting that an ultrasound transducer located within the vessel lumen delivers energy to a depth of 0.5-9.5 mm. To demonstrate the effect on tissue, ultrasound energy was delivered to *ex vivo* bovine liver sections suspended in a static water bath at a distance of 8 mm. Consistent with computational models, the thermal effect matched the predicted distribution of temperatures >47°C. The cooling effect of the water interface prevented an effect at the water-tissue interface **(Figure 3B)**.

ULTRASOUND PULMONARY ARTERY DENERVATION INDUCES ACUTE HISTOLOGICAL CHANGES

To demonstrate the thermal effect on nerves, PDN was performed in domestic swine. Histological examination showed coagulation of collagenous connective and adipose tissue, and coagulation,

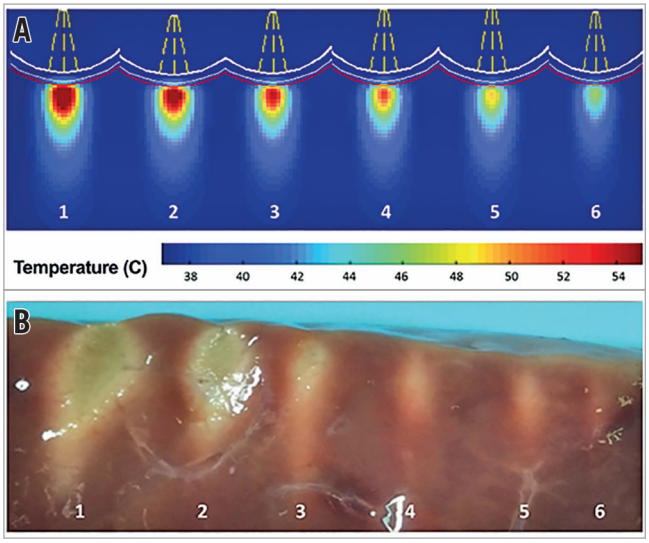

Figure 3. *The thermal effect of ultrasound energy delivery in tissue. A) Computational simulation of the thermal effect to tissue following exposure to varied ultrasonic intensities. B) Thermal effect in bovine liver following ultrasonic energy delivery (white-thermal effect).*

vacuolation and pyknosis nerves **(Figure 4A-Figure 4C)** indicating an acute localised thermal effect.

ULTRASOUND PULMONARY ARTERY DENERVATION REDUCES PULMONARY ARTERIAL PRESSURE

Administration of TxA2 resulted in the development of acute pulmonary hypertension in domestic swine, as demonstrated by a mean pulmonary artery pressure (mPAP) greater than 40 mmHg in both the control and PDN groups **(Figure 5)**. PDN was performed following the first TxA2 challenge. In the control group, the achieved mPAP response was consistent between the first and second TxA2 infusions. PDN reduced mPAP during the second TxA2 challenge when compared to the sham control group **(Figure 5)**. No significant effect was observed on systemic blood pressure or heart rate.

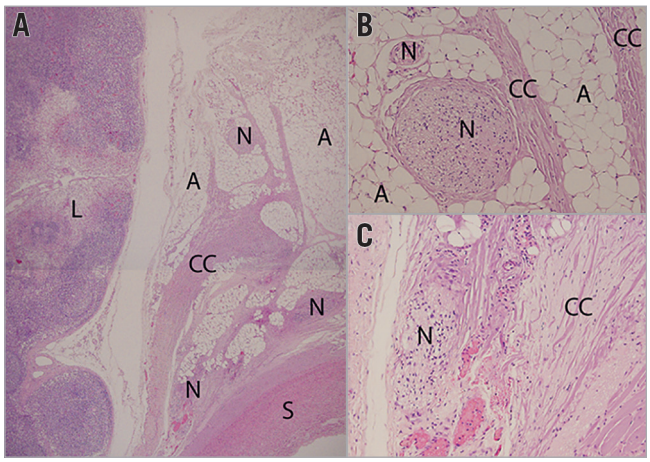

Figure 4. *The acute effect of ultrasound PDN. A) - C) H&E stained sections demonstrate thermal effect indicated by coagulation of collagenous tissue and nuclei pyknosis of cells including nerves. The intima and media are spared as are local lymph nodes (A: adipose, CC: coagulated collagen, L: lymph, N: nerve and S: smooth muscle cells).*

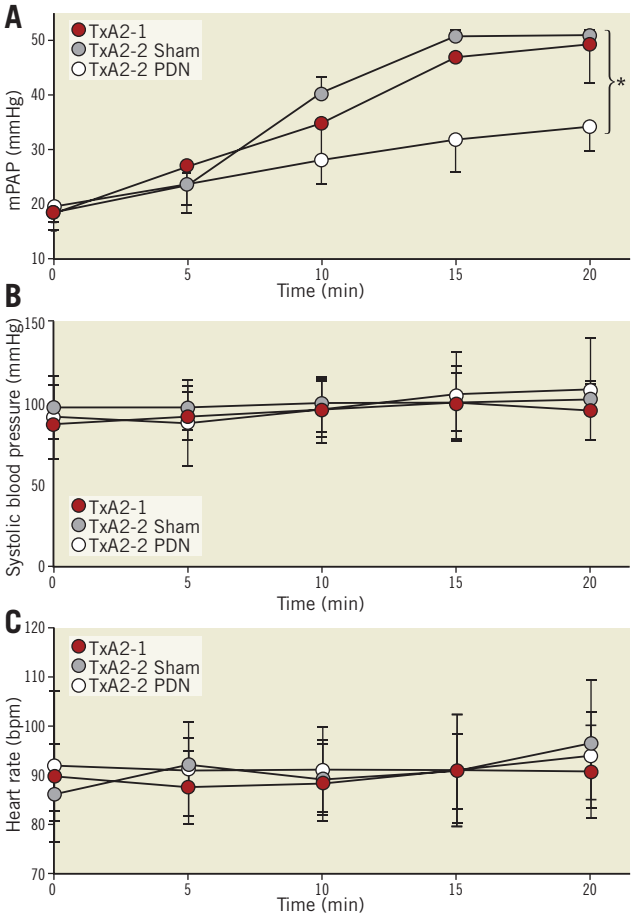

Figure 5. *Ultrasound PDN reduces TxA2 induced PH. Mean pulmonary artery pressure (A), systolic blood pressure (B) and heart rate (C) in sham and PDN treated animals (mean±SD, *p<0.05, Student's t-test).*

SAFETY

No pulmonary artery dissection, perforation or rupture was identified, and no charring or thrombus formation was present during the studies. The animals were kept under surveillance for 14, 28 and 95 days post PDN. No abnormalities were identified in routine blood investigations, activity or weight gain, and no cardiorespiratory distress was identified **(Supplementary Table 1)**.

DURATION OF HISTOLOGICAL CHANGES FOLLOWING PDN

To determine the long-term effect of ultrasound PDN on the vessel wall, histological examination was undertaken in treated animals at 14, 28 and 95 days. Macroscopic assessment showed no damage to the heart, no pulmonary artery thrombus or charring, and no aneurysm, dissection, perforation or stenosis of the

pulmonary arteries or the adjacent aorta. Focal areas of neointima 150-250 µm in depth were present **(Supplementary Figure 1)** with no evidence of lumen reduction (defined as a cross-sectional reduction >5%). Within the adventitia, localised areas of fibrosis affecting connective, adipose and nerve tissue were observed at days 14, 28 and 95 days post PDN at a depth of 0.5-9.5 mm **(Figure 6, Figure 7, Supplementary Table 2)**. The presence of giant cells, eosinophils and neutrophils at day 14 demonstrated an early inflammatory response, which was no longer present at 95 days. Large orbicular lipid droplets indicated a thermal effect in adipose tissue, while the fibrosis and thickening of the epineurium persisted to 95 days post PDN, indicating long-term alteration of the nerve structure **(Figure 6, Figure 7, Supplementary Table 2)**. TH staining was reduced 95 days post PDN, demonstrating a long-term effect on sympathetic nerves (**Figure 8**, 0.190.09 vs 0.050.03, p<0.0001). Histological examination of adjacent structures including the lungs and aorta demonstrated no thermal effect.

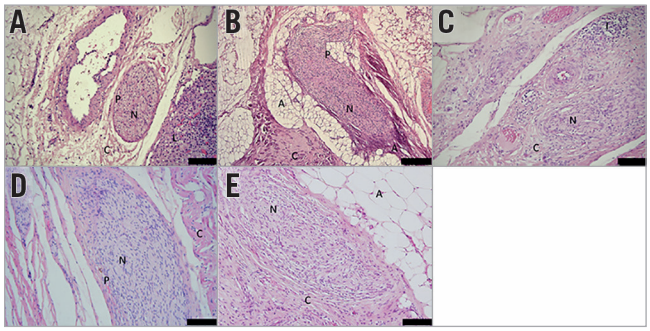

Figure 6. *Time course of thermal injury following PDN. A) Control. B) Acute thermal effect with coagulation of nerve and collagenous connective tissue. C) - E) Day 14, day 28 and day 95. Ultrasound PDN is associated with long-term endoneural changes of nerves in the pulmonary artery adventitia demonstrated by the increased cellularity, perineuronal inflammation and fibrosis (H&E stained sections; A: adipose tissue; C: collagenous connective tissue, N: nerve; P: epineurium).*

Discussion

The lungs and pulmonary vasculature release and metabolise >40% of circulating norepinephrine[30]. Sympathetic activity is increased in patients with PAH[5] and identifies patients with an adverse prognosis[6]. These findings suggest that sympathetic modulation may be a potential target for treatment of PAH.

Neurohormonal modulation is an established strategy for the treatment of heart failure, reducing morbidity and mortality[8-13]. An 18-patient trial of bisoprolol in patients with idiopathic PAH reduced heart rate and increased stroke volume; however, it reduced cardiac output and the six-minute walk test[17]. As such, targeting nerves that supply the pulmonary vasculature without an adverse effect on cardiac function is an attractive concept. Percutaneous technologies developed for renal denervation reduce systemic blood pressure in patients with hypertension both off[31,32] and on[33] antihypertensive medication in randomised, sham-controlled studies and provide the opportunity to investigate the effect of denervation of the pulmonary artery for the treatment of pulmonary hypertension.

In humans, the pulmonary arteries are supplied by a predominantly sympathetic innervation (71%) that is circumferential in distribution with 40% at the left and right pulmonary arteries at a depth >4 mm. Computational modelling and *ex vivo* studies demonstrated delivery of ultrasonic energy in tissue to a depth of

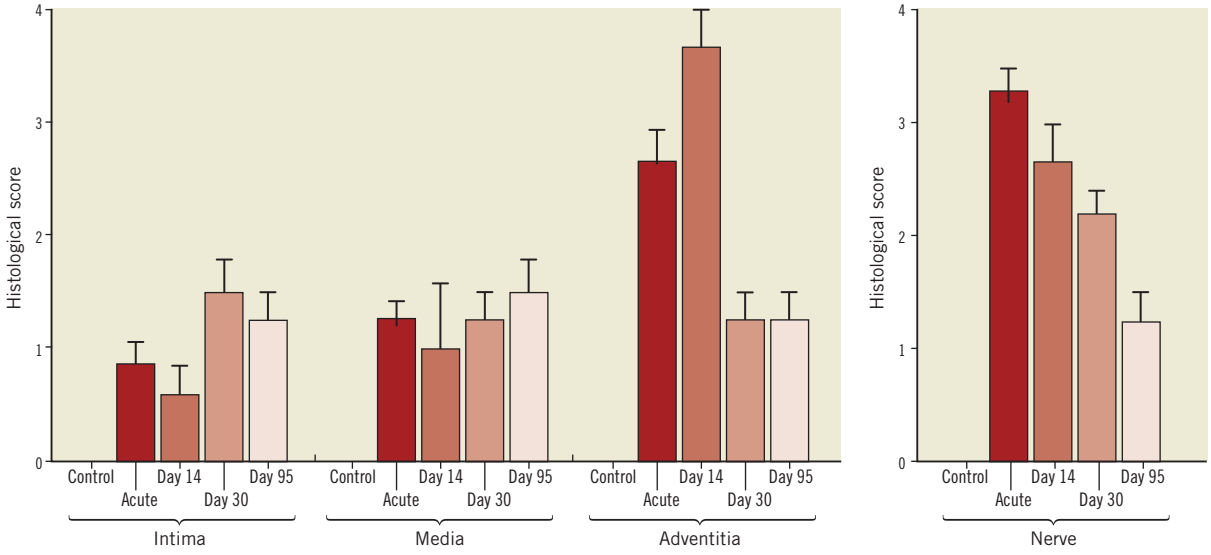

Figure 7. *Quantification of vessel and nerve injury following ultrasound PDN. Vessel scoring quantified endothelial loss, medial injury, inflammation, soft tissue injury and necrosis (0-none to 4-severe). Nerve scoring quantified perineural inflammation or fibrosis and endoneural injury including vacuolisation, digestion chambers, pyknotic nuclei, and necrosis (0-none to 4-severe).*

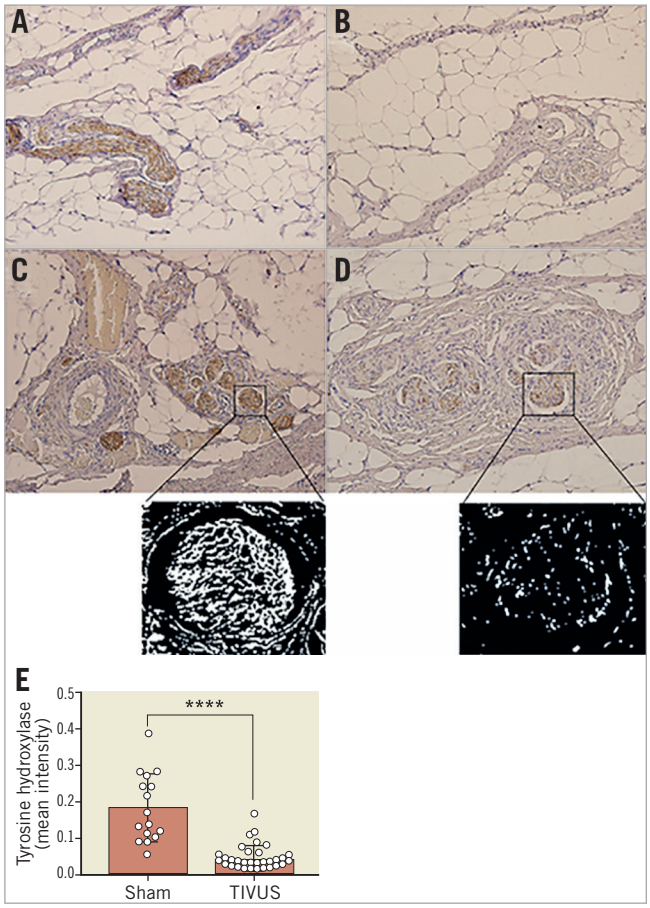

Figure 8. *Ultrasound PDN results in reduced tyrosine hydroxylase staining at 95 days post procedure. Tyrosine hydroxylase (brown) stained pulmonary artery nerve sections at day 95. A) Control. B) - D) PDN. Magnified sections of panels C and D represent threshold-adjusted, colour-inverted images used for quantification of TH staining. E) Pulmonary artery nerve TH staining in PDN and sham treated animals (meanSEM, ****p<0.0001, Mann-Whitney test).*

9.5 mm, sparing the tissue-water interface that represents the vessel intima and media. *In vivo* histological alterations of nerves in the pulmonary artery adventitia following ultrasonic PDN were consistent with previous reports of radio-frequency (RF) renal[28] and pulmonary[20] denervation with altered structure, demyelination and reduced TH immunostaining[21]. RF energy results in local energy delivery altering the histological structure of the intima, media and adventitia to a depth of ~3 mm[20,21]. The present study demonstrates histological changes to nerves at a depth of 9.5 mm with limited effects on the pulmonary artery intima and media. This may be of benefit in patients with PAH in whom the media is thickened and the distance from the lumen to the adventitia is increased[34].

Incomplete ablation has been proposed as a potential mechanism of failure in renal denervation. The TIVUS system provides a semi-circumferential energy delivery with three externally directed beams. *In vivo* studies have demonstrated that a three-directional ultrasound probe in a 2.5 cm pulmonary artery results in structural alteration of ~80% of the vessel circumference **(Supplementary Figure 2)**. We used human anatomical data to develop a structured procedure to target the majority of the pulmonary vascular innervation through multiple activations, similar to techniques used to provide a "complete" renal ablation.

Consistent with prior reports of RF-based denervation in balloon-distension[19], TxA2[20] and monocrotaline[21] models of PH, ultrasound PDN improved pulmonary haemodynamics in an acute vasoconstrictive model of PH as demonstrated by a reduction in mPAP. Histological evidence of denervation following ultrasound energy delivery was present 95 days post PDN with altered nerve structure and staining to a depth of 9.5 mm. These data suggest that ultrasound energy delivery may target a greater proportion of the nerves innervating the pulmonary vasculature than RF energy. No arrhythmias or significant changes in heart rate or systemic pressure were identified during follow-up. The left and right ventricles are interdependent, and at increased right-sided pressure the interventricular septum displaces leftward, altering the shape, filling and function of the left ventricle. This effect may mask physiological effects of PDN on systemic pressure in models with increased right-sided pressures.

The first clinical study of PDN in patients with idiopathic PAH provided early evidence of clinical benefit[22]. Subsequent reports have broadened the patient groups treated, providing further promising results[35]. These studies are single-centre and limited in patient number. Due to study design, there are to date few data to inform understanding of the longevity of the haemodynamic improvements identified or provide evidence of a therapeutic effect in patients treated with PAH-specific therapies.

Strengths and limitations

PAH in humans is driven by pulmonary vascular remodelling and vasoconstriction. Acute haemodynamic changes in the TxA2 model suggest that ultrasound PDN modulates pulmonary vasoconstriction, but provide no data relating to remodelling. The demonstration of altered nerve structure and staining *in vivo* and the description of the anatomical distribution of nerves around the pulmonary vasculature in humans demonstrate that nerves supplying the pulmonary vasculature are accessible via a percutaneous ultrasound-based procedure. As such, these data provided a basis for clinical studies of ultrasound pulmonary artery denervation in PAH, a condition for which all disease-specific therapies target vasoconstriction[1].

Conclusions

The present study describes the distribution of innervation of the proximal pulmonary vasculature and demonstrates that ultrasonic energy delivered by a percutaneous catheter-based system results in sustained alteration in the structure and histochemical staining of sympathetic nerves, sparing the vessel intima and media. Additionally, ultrasound PDN reduced mPAP in an acute porcine model of PH.

Impact on daily practice

Patients with pulmonary arterial hypertension continue to experience significant morbidity and mortality. Therapeutic intravascular ultrasound pulmonary artery denervation alters nerve structure and reduces pulmonary artery pressure in animal models of pulmonary hypertension. Further clinical studies are required to determine efficacy in patients with pulmonary arterial hypertension.

Acknowledgements

A.R. Tzafriri thanks Fernando Garcia-Polite (CBSET) for technical support.

Funding

Studies were funded by SoniVie, Israel. A. Rothman is supported by a Wellcome Trust grant (206632/Z/17/Z).

Conflict of interest statement

A. Rothman, M. Jonas, M. Leon, O. Ben-Yehuda and L. Rubin have consulted for SoniVie. D. Shav is employed by SoniVie. A.R. Tzafriri, D. Castel, and H. Traxler report grants from SoniVie.

References

1. Galiè N, Humbert M, Vachiery JL, Gibbs S, Lang I, Torbicki A, Simonneau G, Peacock A, Vonk Noordegraaf A, Beghetti M, Ghofrani A, Gomez Sanchez MA, Hansmann G, Klepetko W, Lancellotti P, Matucci M, McDonagh T, Pierard LA, Trindade PT, Zompatori M, Hoeper M; ESC Scientific Document Group. 2015 ESC/ERS Guidelines for the diagnosis and treatment of pulmonary hypertension: The Joint Task Force for the Diagnosis and Treatment of Pulmonary Hypertension of the European Society of Cardiology (ESC) and the European Respiratory Society (ERS): Endorsed by: Association for European Paediatric and Congenital Cardiology (AEPC), International Society for Heart and Lung Transplantation (ISHLT). *Eur Heart J.* 2016;37:67-119.

2. Galiè N, Corris PA, Frost A, Girgis RE, Granton J, Jing ZC, Klepetko W, McGoon MD, McLaughlin VV, Preston IR, Rubin LJ, Sandoval J, Seeger W, Keogh A. Updated treatment algorithm of pulmonary arterial hypertension. *J Am Coll Cardiol.* 2013;62:D60-72.

3. Van Albada ME, Loot FG, Fokkema R, Roofthooft MT, Berger RM. Biological serum markers in the management of pediatric pulmonary arterial hypertension. *Pediatr Res.* 2008;63:321-7.

4. Nootens M, Kaufmann E, Rector T, Toher C, Judd DD, Francis GS, Rich S. Neurohormonal activation in patients with right ventricular failure from pulmonary hypertension: relation to hemodynamic variables and endothelin levels. *J Am Coll Cardiol.* 1995;26:1581-5.

5. Velez-Roa S, Ciarka A, Najem B, Vachiery JL, Naeije R, van de Borne P. Increased sympathetic nerve activity in pulmonary artery hypertension. *Circulation.* 2004;110:1308-12.

6. Ciarka A, Doan V, Velez-Roa S, Naeije R, van de Borne P. Prognostic significance of sympathetic nervous system activation in pulmonary arterial hypertension. *Am J Respir Crit Care Med.* 2010;181:1269-75.

7. de Man FS, Handoko ML, Guignabert C, Bogaard HJ, Vonk-Noordegraaf A. Neurohormonal axis in patients with pulmonary arterial hypertension: friend or foe? *Am J Respir Crit Care Med.* 2013;187:14-9.

8. Packer M, Coats AJ, Fowler MB, Katus HA, Krum H, Mohacsi P, Rouleau JL, Tendera M, Castaigne A, Roecker EB, Schultz MK, DeMets DL; Carvedilol Prospective Randomized Cumulative Survival Study Group. Effect of carvedilol on survival in severe chronic heart failure. *N Engl J Med.* 2001;344:1651-8.

9. [No authors listed]. The Cardiac Insufficiency Bisoprolol Study II (CIBIS-II): a randomised trial. *Lancet.* 1999;353:9-13.

10. [No authors listed]. Effect of metoprolol CR/XL in chronic heart failure: Metoprolol CR/XL Randomised Intervention Trial in Congestive Heart Failure (MERIT-HF). *Lancet.* 1999;353:2001-7.

11. CONSENSUS Trial Study Group. Effects of enalapril on mortality in severe congestive heart failure. results of the Cooperative North Scandinavian Enalapril Survival Study (CONSENSUS). *N Engl J Med.* 1987;316:1429-35.

12. SOLVD Investigators, Yusuf S, Pitt B, Davis CE, Hood WB, Cohn JN. Effect of enalapril on survival in patients with reduced left ventricular ejection fractions and congestive heart failure. *N Engl J Med.* 1991;325:293-302.

13. Cohn JN, Johnson G, Ziesche S, Cobb F, Francis G, Tristani F, Smith R, Dunkman WB, Loeb H, Wong M, et al. A comparison of enalapril with hydralazine-isosorbide dinitrate in the treatment of chronic congestive heart failure. *N Engl J Med.* 1991;325:303-10.

14. Perros F, Ranchoux B, Izikki M, Bentebbal S, Happé C, Antigny F, Jourdon P, Dorfmüller P, Lecerf F, Fadel E, Simonneau G, Humbert M, Bogaard HJ, Eddahibi S. Nebivolol for improving endothelial dysfunction, pulmonary vascular remodeling, and right heart function in pulmonary hypertension. *J Am Coll Cardiol.* 2015;65:668-80.

15. de Man FS, Handoko ML, van Ballegoij JJM, Schalij I, Bogaards SJP, Postmus PE, van der Velden J, Westerhof N, Paulus WJ, Vonk-Noordegraaf A. Bisoprolol delays progression towards right heart failure in experimental pulmonary hypertension. *Circ Heart Fail.* 2012;5:97-105.

16. Thenappan T, Roy SS, Duval S, Glassner-Kolmin C, Gomberg-Maitland M. β-blocker therapy is not associated with adverse outcomes in patients with pulmonary arterial hypertension: a propensity score analysis. *Circ Heart Fail.* 2014;7:903-10.

17. van Campen JS, de Boer K, van de Veerdonk MC, van der Bruggen CE, Allaart CP, Raijmakers PG, Heymans MW, Marcus JT, Harms HJ, Handoko ML, de Man FS, Noordegraaf AV, Bogaard HJ. Bisoprolol in idiopathic pulmonary arterial hypertension: an explorative study. *Eur Respir J.* 2016;43:787-96.

18. Bandyopadhyay D, Bajaj NS, Zein J, Minai OA, Dweik RA. Outcomes of β-blocker use in pulmonary arterial hypertension: a propensity-matched analysis. *Eur Respir J.* 2015;46:750-60.

19. Chen SL, Zhang YJ, Zhou L, Xie DJ, Zhang FF, Jia HB, Wong SS, Kwan TW. Percutaneous pulmonary artery denervation completely abolishes experimental pulmonary arterial hypertension in vivo. *EuroIntervention.* 2013;9:269-76.

20. Rothman AM, Arnold ND, Chang W, Watson O, Swift AJ, Condliffe R, Elliot CA, Kiely DG, Suvarna SK, Gunn J, Lawrie A. Pulmonary artery denervation reduces pulmonary artery pressure and induces histological changes in an acute porcine model of pulmonary hypertension. *Circ Cardiovasc Interv.* 2015;8:e002569.

21. Zhou L, Zhang J, Jiang XM, Xie DJ, Wang JS, Li L, Li B, Wang ZM, Rothman AMK, Lawrie A, Chen SL. Pulmonary Artery Denervation Attenuates Pulmonary Arterial Remodeling in Dogs With Pulmonary Arterial Hypertension Induced by Dehydrogenized Monocrotaline. *JACC Cardiovasc Interv.* 2015;8:2013-23.

22. Chen SL, Zhang FF, Xu J, Xie DJ, Zhou L, Nguyen T, Stone GW. Pulmonary artery denervation to treat pulmonary arterial hypertension: the single-center, prospective, first-in-man PADN-1 study (first-in-man pulmonary artery denervation for treatment of pulmonary artery hypertension). *J Am Coll Cardiol.* 2013;62:1092-100.

23. Fujisawa T, Kataoka M, Kawakami T, Isobe S, Nakajima K, Kunitomi A, Kashimura S, Katsumata Y, Nishiyama T, Kimura T, Nishiyama N, Aizawa Y, Murata M, Fukuda K, Takatsuki S. Pulmonary Artery Denervation by

Determining Targeted Ablation Sites for Treatment of Pulmonary Arterial Hypertension. *Circ Cardiovasc Interv.* 2017;10:e005812.

24. Dewhirst MW, Viglianti BL, Lora-Michiels M, Hanson M, Hoopes PJ. Basic principles of thermal dosimetry and thermal thresholds for tissue damage from hyperthermia. *Int J Hyperthermia.* 2003;19:267-94.

25. Giering K, Lamprecht I, Minet O, Handke A. Determination of the specific heat capacity of healthy and tumorous human tissue. *Thermochimica Acta.* 1995;251:199-205.

26. Roehl AB, Steendijk P, Baumert JH, Schnoor J, Rossaint R, Hein M. Comparison of 3 methods to induce acute pulmonary hypertension in pigs. *Comp Med.* 2009;59:280-6.

27. Sakakura K, Ladich E, Cheng Q, Otsuka F, Yahagi K, Fowler DR, Kolodgie FD, Virmani R, Joner M. Anatomic assessment of sympathetic peri-arterial renal nerves in man. *J Am Coll Cardiol.* 2014;64:635-43.

28. Sakakura K, Ladich E, Edelman ER, Markham P, Stanley JR, Keating J, Kolodgie FD, Virmani R, Joner M. Methodological standardization for the pre-clinical evaluation of renal sympathetic denervation. *JACC Cardiovasc Interv.* 2014;7:1184-93.

29. Lamprecht MR, Sabatini DM, Carpenter AE. CellProfiler: free, versatile software for automated biological image analysis. *Biotechniques.* 2007;42:71-5.

30. Esler M, Willett I, Leonard P, Hasking G, Johns J, Little P, Jennings G. Plasma noradrenaline kinetics in humans. *J Auton Nerv Syst.* 1984;1:125-44.

31. Townsend RR, Mahfoud F, Kandzari DE, Kario K, Pocock S, Weber MA, Ewen S, Tsioufis K, Tousoulis D, Sharp ASP, Watkinson AF, Schmieder RE, Schmid A, Choi JW, East C, Walton A, Hopper I, Cohen DL, Wilensky R, Lee DP, Ma A, Devireddy CM, Lea JP, Lurz PC, Fengler K, Davies J, Chapman N, Cohen SA, DeBruin V, Fahy M, Jones DE, Rothman M, Böhm M; SPYRAL HTN-OFF MED trial investigators*. Catheter-based renal denervation in patients with uncontrolled hypertension in the absence of antihypertensive medications (SPYRAL HTN-OFF MED): a randomised, sham-controlled, proof-of-concept trial. *Lancet.* 2017;390:2160-70.

32. Azizi M, Schmieder RE, Mahfoud F, Weber MA, Daemen J, Davies J, Basile J, Kirtane AJ, Wang Y, Lobo MD, Saxena M, Feyz L, Rader F, Lurz P, Sayer J, Sapoval M, Levy T, Sanghvi K, Abraham J, Sharp ASP, Fisher NDL, Bloch MJ, Reeve-Stoffer H, Coleman L, Mullin C, Mauri L; RADIANCE-HTN Investigators. Endovascular ultrasound renal denervation to treat hypertension (RADIANCE-HTN SOLO): a multicentre, international, single-blind, randomised, sham-controlled trial. *Lancet.* 2018;391:2335-45.

33. Kandzari DE, Böhm M, Mahfoud F, Townsend RR, Weber MA, Pocock S, Tsioufis K, Tousoulis D, Choi JW, East C, Brar S, Cohen SA, Fahy M, Pilcher G, Kario K; SPYRAL HTN-ON MED Trial Investigators. Effect of renal denervation on blood pressure in the presence of antihypertensive drugs: 6-month efficacy and safety results from the SPYRAL HTN-ON MED proof-of-concept randomised trial. *Lancet.* 2018;391:2346-55.

34. Prapa M, McCarthy KP, Dimopoulos K, Sheppard MN, Krexi D, Swan L, Wort SJ, Gatzoulis MA, Ho SY. Histopathology of the great vessels in patients with pulmonary arterial hypertension in association with congenital heart disease: large pulmonary arteries matter too. *Int J Cardiol.* 2013;168:2248-54.

35. Chen SL, Zhang H, Xie DJ, Zhang J, Zhou L, Rothman AM, Stone GW. Hemodynamic, functional, and clinical responses to pulmonary artery denervation in patients with pulmonary arterial hypertension of different causes: phase II results from the Pulmonary Artery Denervation-1 Study. *Circ Cardiovasc Interv.* 2015;8:e002837.

Supplementary data

Supplementary Figure 1. Haematoxylin and eosin stained sections of pulmonary artery at points of ultrasound energy delivery showing the neointima found in the chronic treated animals at 28 and 95 days post treatment.

Supplementary Figure 2. Haematoxylin and eosin stained section of a left pulmonary artery following a single activation of a 3-directional TIVUS catheter. Black outline indicates areas of acute histological alteration.

Supplementary Table 1. Physical and biochemical characteristics of domestic swine following pulmonary artery denervation.

Supplementary Table 2. Pulmonary artery nerve depth and area.

The supplementary data are published online at: https://eurointervention.pcronline.com/doi/10.4244/EIJ-D-18-01082

Supplementary data

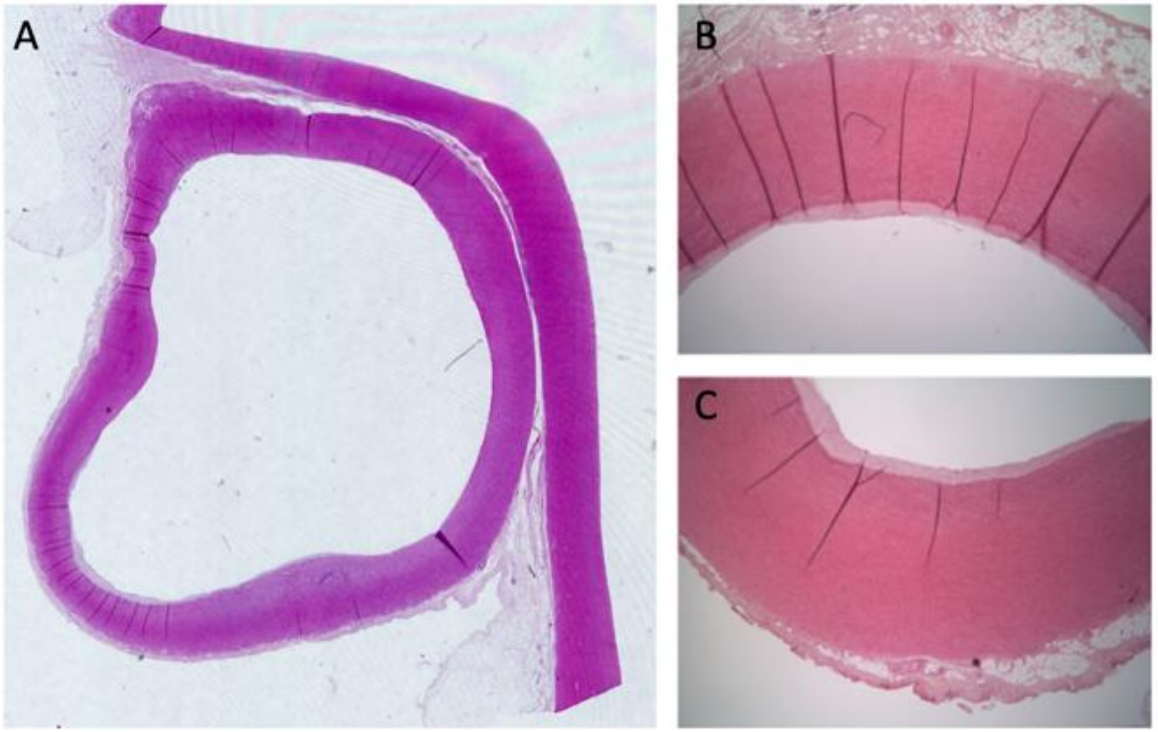

Supplementary Figure 1. Haematoxylin and eosin stained sections of pulmonary artery at points of ultrasound energy delivery showing the neointima found in the chronic treated animals at 28 and 95 days post treatment.

A) Microphotograph of the main pulmonary artery slide from a treated animal, following 28 days of surveillance.

B) & C) x20 magnification of the main pulmonary artery from a treated animal, following 28 days of surveillance.

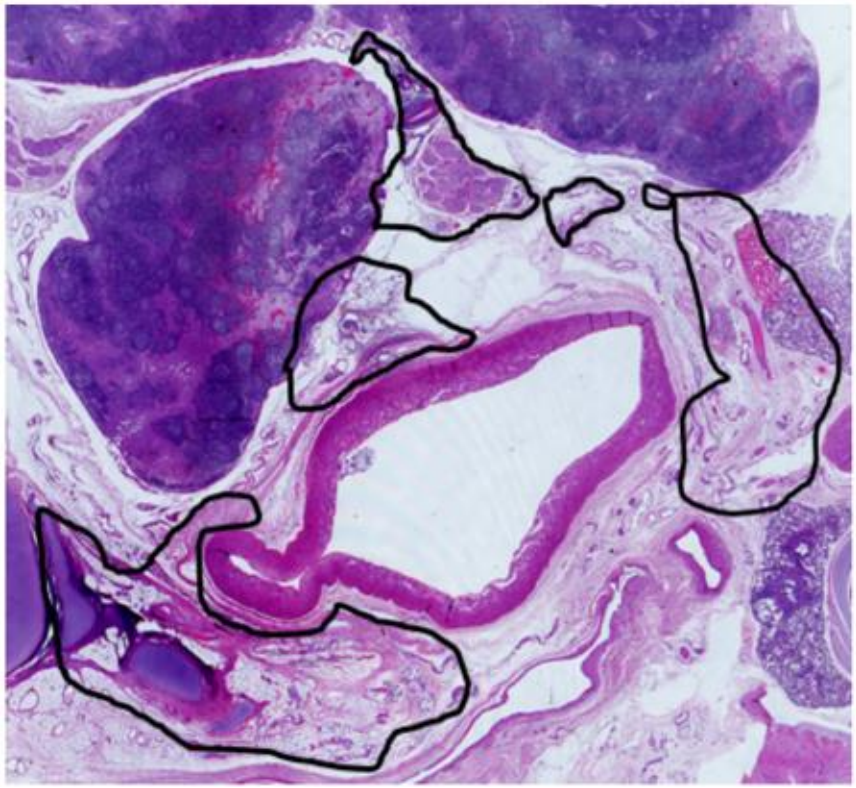

Supplementary Figure 2. Haematoxylin and eosin stained section of a left pulmonary artery following a single activation of a 3-directional TIVUS catheter. Black outline indicates areas of acute histological alteration.

Supplementary Table 1. Physical and biochemical characteristics of domestic swine following pulmonary artery denervation.

Parameter		Time of measure					
		Pre-denervation (mean, SD)	**Post-denervation (mean, SD)**	**Sham (mean, SD)**	**Day 14 (mean, SD)**	**Day 28 (mean, SD)**	**Day 95 (mean, SD)**
Weight	(kg)	72.4 (1.2)	NA	74.0 (1.4)	75.5 (1.2)	80.1 (2.7)	118.2 (7.2)
HR	(BPM)	88.3 (9.4)	NA	81.0 (12.7)	91 (12.2)	NA	68.5 (12.5)
ECG		Normal	Normal	Normal	Normal	Normal	Normal
Lung auscultation		Normal	Normal	Normal	Normal	Normal	Normal
White blood cells	(6.7-22.8 10^3/ul)	18.9 (5.7)	NA	NA	23.1 (1.4)	14.1 (2.1)	13.8 (1.4)
Red blood cells	(5.6-8.8 10^6/ul)	6.4 (0.6)	NA	NA	7.1 (1.1)	6.5 (0.5)	6.4 (0.3)
Haemoglobin	(10.1-15.1 g/dL)	10.3 (1.2)	NA	NA	10.6 (0.7)	10.9 (0.6)	10.7 (0.5)
Platelets	(147-704 10^3/ul)	322.4 (28.3)	NA	NA	297.5 (60.0)	390.0 (58.7)	356.8 (97.4)
Creatinine	(0.75-1.7 mg/dL)	1.3 (0.1)	NA	NA	1.3 (0.2)	1.5 (0.1)	1.9 (0.3)
Urea	(5-61 mg/dL)	20.9 (3.8)	NA	NA	19.7 (4.0)	25.4 (5.2)	24.6 (5.1)
Sodium	(136-147 mmol/L)	140.9 (3.2)	NA	NA	140.0 (1.6)	139.8 (1.5)	138.8 (2.2)
Potassium	(2.8-6.2 mmol/L)	4.5 (0.3)	NA	NA	6.1 (0.4)	4.2 (0.2)	4.1 (0.3)

Supplementary Table 2. **Pulmonary artery nerve depth and area.**

A. Depth and area of neurofilament positive nerves (all nerves) adjunct to the main (MPA), left (LPA) and right (RPA) pulmonary arteries.

Artery	Cumulative nerve area (mm^2)	Averaged nerve area (mm^2)	STDEV (mm^2)	% of nerves at distance >4 mm	% of nerves at distance >5 mm	% of nerves at distance >7.5 mm	% of nerves at distance >10 mm
MPA	7.8	0.11	0.26	21.7	10.1	1.4	0.0
LPA	2.5	0.06	0.11	44.7	36.8	13.2	5.3
RPA	3.4	0.07	0.14	46.2	25.0	9.6	0.0

.

B. Depth and area of tyrosine hydroxylase positive staining (sympathetic nerves) of nerves adjunct to the main (MPA), left (LPA) and right (RPA) pulmonary arteries.

Artery	Cumulative nerve area (mm^2)	Averaged nerve area (mm^2)	STDEV (mm^2)	% of nerves at distance >4 mm	% of nerves at distance >5 mm	% of nerves at distance >7.5 mm	% of nerves at distance >10 mm
MPA	4.8	0.22	0.30	9.1	0.0	0.0	0
LPA	1.9	0.13	0.19	27.3	22.7	9.1	0
RPA	2.6	0.16	0.21	50.0	36.4	0.0	0

C. Pulmonary artery vessel size and percent area and number of tyrosine hydroxylase positive (sympathetic) relative to neurofilament positive nerves (total) by depth from luminal aspect of the main (MPA), left (LPA) and right (RPA) pulmonary arteries.

Artery	Vessel diameter (mm)	Intima to adventitia (intima + media, mm)	Tyrosine hydroxylase positive nerve area (percentage by total nerve area)	Tyrosine hydroxylase positive nerves (percentage by nerve number)	% of nerves at depth >4 mm	% of nerves at depth >5 mm
MPA	16	1.1	60.9	31.9	13.3	0.0
LPA	14	1.1	77.9	39.5	35.3	35.7
RPA	10	1.1	75.0	30.8	45.8	61.5